Jitong Zhao, Marco Liebscher, Albert Michel, Dominik Junger, Ana Carolina Constâncio Trindade, Fláviode Andrade Silva Viktor Mechtcherine

Development and testing of fast curing, mineral-impregnated carbon fiber (MCF) reinforcements based on metakaolin-made geopolymers

Erstveröffentlichung in / First published in:

Cement and Concrete Composites. 2021, 116, Art. Nr. 103898. Elsevier. ISSN 0958-9465.

DOI: https://doi.org/10.1016/j.cemconcomp.2020.103898

Development and testing of fast curing, mineral-impregnated carbon-fiber (MCF) reinforcements based on metakaolin-made geopolymers

Jitong Zhao[1], Marco Liebscher[1], Albert Michel[1], Dominik Junger[1], Ana Carolina Constâncio Trindade[2], Flávio de Andrade Silva[2], Viktor Mechtcherine[1]

1- Technische Universität Dresden, Institute of Construction Materials, 01062 Dresden, Germany
2- Pontifícia Universidade Católica do Rio de Janeiro, Department of Civil and Environmental Engineering, 22451-900, Rio de Janeiro, Brazil

Abstract:

Mineral-impregnated, carbon-fiber composites (MCF) are a promising alternative to conventional concrete reinforcements. For the efficient industrial production of MCF, sufficient processing time for the impregnation suspension must be ensured. In the present investigation, a metakaolin-made geopolymer (GP) has been developed and tested for this purpose. The impregnation of carbon-fiber yarns was performed continuously and automated. Subsequently, the MCF were heat-treated at 75 °C to accelerate the reaction processes. The mechanical performance of MCF gradually increased in the advancement of the curing process from 2 to 8 hours, which is attributed to the greater extent of geopolymerization. In such extended curing, thermogravimetric and microscopic analysis showed indeed a more "reacted" microstructure but also a higher content of voids. After heating for 8 hours, the tensile strength and Young's modulus of MCF reached 2960 MPa and 259 GPa, respectively, when related to the yarn cross-sectional area.

Keywords: carbon-fiber composite; mineral impregnation; geopolymer; reinforcement; automated processing.

1. Introduction

The use of carbon fiber (CF) as reinforcement in concrete construction has attracted much attention in recent years due to its lightweight, superior mechanical properties, and, most particularly, much higher corrosion resistance when compared to conventional steel reinforcement. These features enable the saving of raw materials while manufacturing lightweight, durable structures [1–3]. To produce a CF reinforcement, unidirectional CF multi-filaments are usually bundled to textile reinforcement or to rebars and then impregnated (coated) with a thermoplastic or duromeric polymer [4,5]. The polymer matrix enhances the robustness and handling of the reinforcement considerably. But primarily it ensures the adequate transfer of load both from the surrounding concrete to the outer CF filaments and, in turn, from the outer filaments to those in the interior [6,7].

While polymer impregnation in this realm is the state-of-the-art technology, the low thermal resistance of polymer matrices, as well as the relatively weak bond between composite reinforcement, i.e., carbon-fiber-reinforced polymer (CFRP), and concrete matrix, hinder the broad practical application of carbon concrete composites in construction, especially in cases when fire resistance is required [8]. At elevated temperatures, the polymers soften or thermally decompose, resulting in the complete loss of their load-bearing capacity and thus the intended function of CFRP [9–13]. For instance, Katz *et al.* [10] demonstrated a loss of nearly 90% in the bond strength of FRP bars to the surrounding concrete on a temperature increase to 200 °C.

In overcoming this hurdle thermally stable, mineral-impregnated, carbon-fiber composites (MCF) have been developed [8,14]. The MCF exhibit highly flexible processability, excellent chemical compatibility between composite and concrete, and high durability when compared to conventional CFRP bars [14,15]. In previous investigations, the CF yarns coated with fine reactive pozzolanic particles, such as silicon oxides, showed enhanced bond properties towards concrete matrix in comparison to yarns without any coating [16–18]. Several subsequent studies on cement-based MCF demonstrated significant enhancement in the mechanical properties,

particularly bond strength, at temperatures of up to 500 °C when compared to polymer-impregnated carbon yarns [8, 19]. The use of a modified magnesia-phosphate cement suspension instead of epoxy resin as coating material was reported by Zhang *et al*. [20] to yield a significant increase in the bond strength of carbon sheets to concrete in a similar temperature range.

While the use of cement-based materials for coating or impregnation yields considerable improvement in the thermal resistance of the composite and its bond to concrete, it poses some limitations with respect to the processing time in the automated, continuous production of MCF. This can be traced back to cement hydration reactions, which lead to a significant increase in the viscosity of the impregnating suspension over short time periods [14]. Moreover, the cement-based matrices require many weeks for sufficient strength development, which is unfavorable in respect of the economic production of MCF.

A promising solution is the use of geopolymer (GP) binders since GP usually yields sufficiently stable rheological properties in the early stages of processing. They often require subsequent thermal curing to accelerate the reaction, similar to many thermosets, allowing fast setting and rapid strength development [21,22]. Thus, a stable continuous manufacturing process over an extended time can be achieved followed by controlled thermal curing. It follows that such a process arrangement would be of great relevance to the industrial production of MCF as a novel reinforcement. Moreover, GP possess excellent mechanical properties over a wide temperature range, which makes them suitable for temperature resistant composites [23].

To date, most publications on fiber-reinforced GP have focused on the incorporation of distinct types of dispersed short fibers [24–27]. Only very few studies have been performed on the use of geopolymer slurries to coat continuous fiber reinforcements, most of them targeting exclusively high-tech applications such as in the automotive or aerospace fields [28–31], few of them aiming at the coating of carbon- or steel-based fabrics for external strengthening existing concrete structures [32,33]. Moreover, the previous investigations were mainly

79 performed on CF reinforcement with a low fiber fineness and rectangular cross-sections, hence,
80 with parameters not favorable to most structural applications. Hung *et al.* [29] used a so-called
81 silica-based geopolymer in combination with carbon 1600 tex 24K fibers and achieved flexural
82 strengths of about 550 MPa after curing at 75 °C for 10 hours. He *et al.* [30] reported flexural
83 strength values ranging from 95 to 234 MPa at various temperatures above 1000 °C. The CF-
84 reinforced GP specimens exhibited high porosity and were produced individually by hand lay-
85 up impregnation of 16 layers. Continuous basalt fibers were coated with GP using hand lay-up
86 to fabricate composites with a flexural strength of approximately 200 MPa [28].
87 Geopolymers can be produced from metakaolin or a range of industrial waste materials such
88 as fly ash and rice rusk ash as well as slag containing abundant aluminosilicates [34].To enable
89 adequate penetration of the mineral suspension into the yarn and a high fiber volume fraction
90 of the composite, the mean particle diameter in the suspension must be in the range of the
91 diameter of the individual CF filaments or even smaller [14]. The diameters of carbon filaments
92 are usually below 10 µm. Highly reactive metakaolin (MK) seems to be a promising candidate
93 for the production of MCF, considering its suitable mean particle size, varying from 1 to 2 µm,
94 its high specific surface area, and its high strength after geopolymer synthesis [35].
95 In the present investigation geopolymer-based impregnated carbon fiber composites were
96 developed, fabricated in a continuous, automated pultrusion process, and cured at 75 °C.
97 Considering the flexible applicability of the newly developed reinforcement after impregnation
98 and relatively brief heat-treatment as key features, this research effort focused on identifying
99 the suitable thermal curing duration at which the best mechanical properties can be achieved.
100 The mechanical properties of the impregnation matrix were evaluated by means of compression
101 and bending tests. After impregnation and following thermal treatment, mercury intrusion
102 porosimetry (MIP), three-point bending tests, and uniaxial tensile tests were conducted to
103 characterize the composites. Finally, a comprehensive electron-microscopic investigation of the
104 composite interphases and the impregnation quality was performed. The results were related to

the mechanical performance observed.

2. Experimental program

2.1 Materials

Highly reactive metakaolin (MK) MetaMax from BASF, Germany, was used as the aluminosilicate precursor due to its high purity and small particle size. Its chemical composition is given in Table 1. To characterize the particle size distribution of the MK powder, a Laser Diffraction Particle Size Analyzer LS 237 from Beckmann Coulter, USA, was used. Fig. 1 shows the particle size distribution of MK ranging from 0.5 to 15 μm. Particle diameters of 10%, 50%, and 90% quantiles were d_{10} = 0.65 μm, d_{50} = 2.84 μm and d_{90} = 9.72 μm, respectively. So seen, almost 80% of MK particles were smaller than the diameter of the carbon filaments used in this investigation, which is approximately 7 μm; as highlighted in red in Fig. 1.

The alkali-based solution, i.e., K-based water glass (WG), was prepared by mixing KOH pellets (Fisher Scientific, Germany), deionized water, and hydrophilic fumed silica (CAB-O-SIL® M-5, CABOT Corporation, Germany) for 24 hours using a magnetic stirrer and a polytetrafluoroethylene (PTFE) magnetic stirring bar. A superplasticizer (SP) (Sapetin, Woellner, Germany) made of phosphonic acids modified by salts was used to increase the flowability to the extent required for the impregnation process. The adequacy of the dispersant with the GP material was demonstrated in a previous study [36].

Table 1. Chemical composition of Metamax MK given by manufacturer.

Oxide composition	***SiO_2***	***Al_2O_3***	***TiO_2***	***Fe_2O_3***	***K_2O***	***MgO***	***CaO***	***Na_2O***	***LOI***
wt%	53.0	43.8	1.70	0.43	0.19	0.03	0.02	0.23	0.46

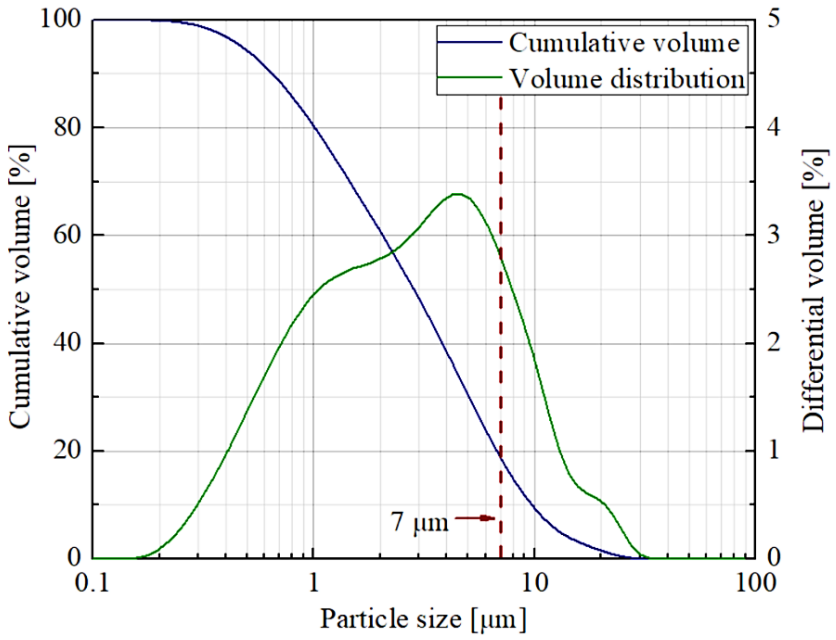

Fig. 1. Particle size distribution curves of metakaolin as measured by laser granulometry.

The commercially available CF roving used in this investigation (SIGRAFIL® C T50-4.4/255-E100, SGL Group, Germany) consists of 50,000 individual filaments, allowing proper comparison with the previously developed cement-based impregnation suspension [14]. The heavy tow roving was sized with epoxy resin and had a fineness of 3,450 tex and a filament diameter of ~7 µm. According to the supplier [37], the tensile strength and modulus of elasticity of the filament are 4400 MPa and 255 GPa, respectively.

2.2 Fabrication of MCF

A geopolymer suspension composed of $SiO_2/Al_2O_3 = 4$, $K_2O/SiO_2 = 0.33$, and $H_2O/K_2O = 8.69$ was prepared by mixing MK powder ($Al_2O_3 \cdot 2SiO_2$), potassium silicate solution ($1.3K_2O \cdot 2SiO_2 \cdot 11.3H_2O$) and the SP by means of a high speed disperser T50 digital ULTRA-TURRAX from IKA at 7000 rpm. This ensured the complete dispersion of the MK particles and a homogeneous suspension of relatively low viscosity. The SP was added into the mixture at a dosage of 4 % by mass of the GP. Table 2 presents the composition of geopolymer suspension for the yarn impregnation. The mixing comprised the following processes described

145 previously [38], where (i) mixing of the MK powder with the alkali solution for 2 min; (ii)
146 addition of the SP; (iii) mixing for another 5 min; and (iv) vibrating the mixture for 10 min to
147 remove entrapped air were performed.
148
149 Table 2. Composition of geopolymer impregnation suspension (considering 1 kg of WG).

Mixture constituent	***Amount [g]***
Metakaolin	538.44
Water glass	1000
Superplasticizer	61.54
WG/MK ratio	1.86

150
151 To ensure the high quality of slurry penetration into the CF yarns, the funnel flow time of
152 30 s and the slump flow of 230 to 240 mm were measured with a small V-funnel having a
153 volume of 150 ml and an opening diameter of 7 mm for the fresh mixture. This special method
154 of studying the viscosity of suspension was used in the development of cement-based
155 impregnation suspensions [19]. The suspension obtained exhibited a sufficient processing
156 window of more than 18 hours for continuous production. The development of the rheological
157 properties of the suspension is to be investigated in detail in a future study.
158 The continuous impregnation of the carbon yarn with the geopolymer suspension was
159 conducted using an automated device consisting of a five-roller-foulard for multiple deflection
160 of the yarn in the suspension, yarn guidance, final shaping, and a hexagonal wheel for
161 deposition of the freshly impregnated yarn; see Fig. 2a. To align the individual filaments over
162 the process line and to avoid the overlapping of the flat yarn, the windings of the reel were
163 straightened over three yarn-guiding levels and an engine-driven kiss-coater. The carbon yarn
164 with a width of ~19 mm was immersed into the geopolymer suspension and deflected five
165 times; see Fig. 2b. The final shaping was carried out using a plastic, funnel-like nozzle with an

opening diameter of 4.1 mm. The samples prepared were assembled on an engine-driven hexagonal wheel by drawing it off under constant tension. A pulling velocity of 360 m/h was set to ensure excellent penetration as well as relatively high processing speed for efficient industrial production in future.

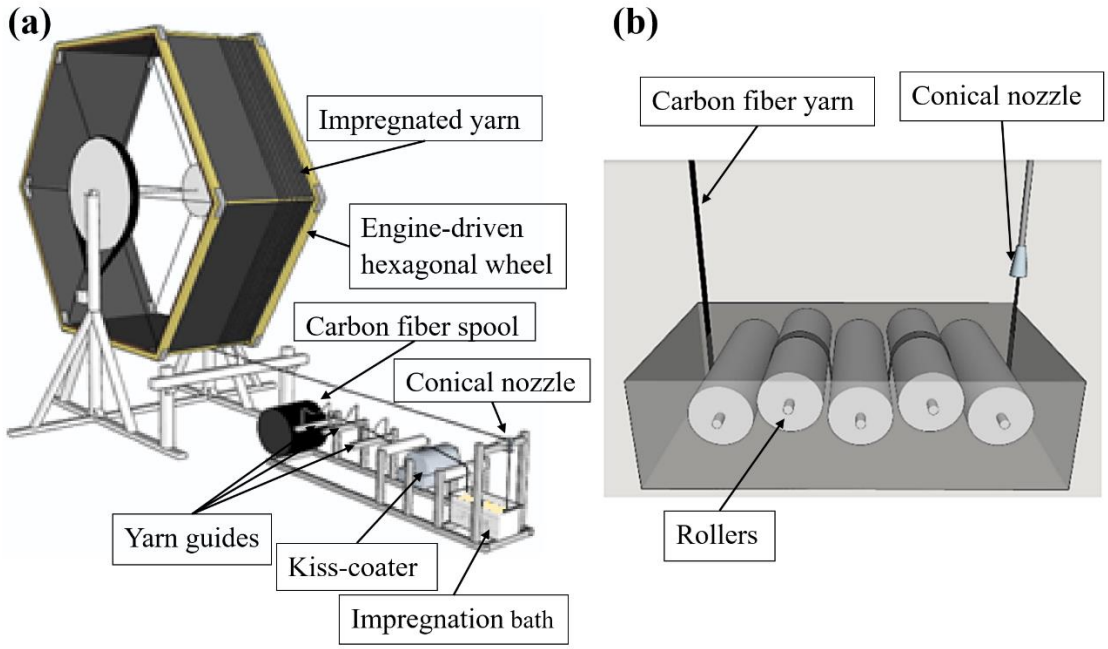

Fig. 2. Schematic drawing of the yarn impregnation device: (a) an overview, (b) processing in a five-roller-foulard, and final shaping.

Following the initial impregnation process, the MCF produced were sealed in a wooden box to prevent water evaporation and then heated in an electrical oven at 75 ℃ over varied curing times of 2, 4, and 8 hours. After heat curing, the specimens were stored under polyethylene foils at 20 °C and 65% relative humidity until testing.

2.3 Testing the geopolymer matrix

To determine the development of the composite matrix's strength at early ages and after 28 days, prismatic samples were prepared with dimensions of 10 mm × 10 mm × 60 mm for bending and compressive tests. The fresh geopolymer mixture was cast into metal molds lined

with semitransparent adhesive tapes and then sealed to prevent early dehydration and cracks in the material, as suggested in a previous study [3838]. The use of a proper curing regime is essential in achieving a chemically reacted geopolymer of high quality. According to the literature, curing temperatures ranging from 40 °C to 85 °C in relatively short timespans of 2 to 48 hours are enough for optimized geopolymerization [39,40错误!未定义书签。].

Hence, one set of specimens was stored at an ambient temperature of 20 °C for 28 days and designated as the reference. Other sets of specimens were treated in the oven at 50 °C and 75 °C for curing durations of 2, 4, and 8 hours. They were demolded after heating and tested immediately, i.e., mere hours after casting. All specimens were kept in dry plastic bags after demolding to prevent early dehydration [41].

Three-point-bending and compressive tests were performed using a Zwick Roell Z1445 machine at a loading rate of 1 mm/min, with load cells of 1 kN and 10 kN, respectively. The flexural strength of the samples was evaluated using a span of 30 mm according to DIN EN 12390-5 [42]. For the compressive test, halves of the remaining flexural samples were used, following DIN EN 12390-3 [43]. Each reported value relates to the average of at least five measurements for both bending and compressive tests.

2.4 Mechanical testing of MCF

The flexural properties and therewith the quality of impregnation of MCF were determined by means of the three-point bending test using a displacement controlled Zwick-Roell testing machine (model ZwickLine) with a span of 100 mm, a displacement rate of 5 mm/min, and a load cell of 1 kN capacity; see Fig. 3a. The bending tests were performed: (i) immediately after the heating process, i.e., just hours after impregnation, and (ii) after additional storing at a temperature of 20 °C and a relative humidity of 55 % at an MCF age of 28 days. Ten specimens were tested for each variation. Fig. 3b shows a readymade bar of MCF produced by metakaolin-made impregnation suspension.

Considering the circumferences of the resulting MCF, the height (h) and width (b) of each composite cross-section were measured individually, while the cross-section was assumed to have an approximately elliptical shape. The maximum flexural stress was calculated according to:

$$\sigma_{max} = \frac{8FL}{\pi b h^2} \quad (1)$$

where F is the maximum measured force and L is the support span.

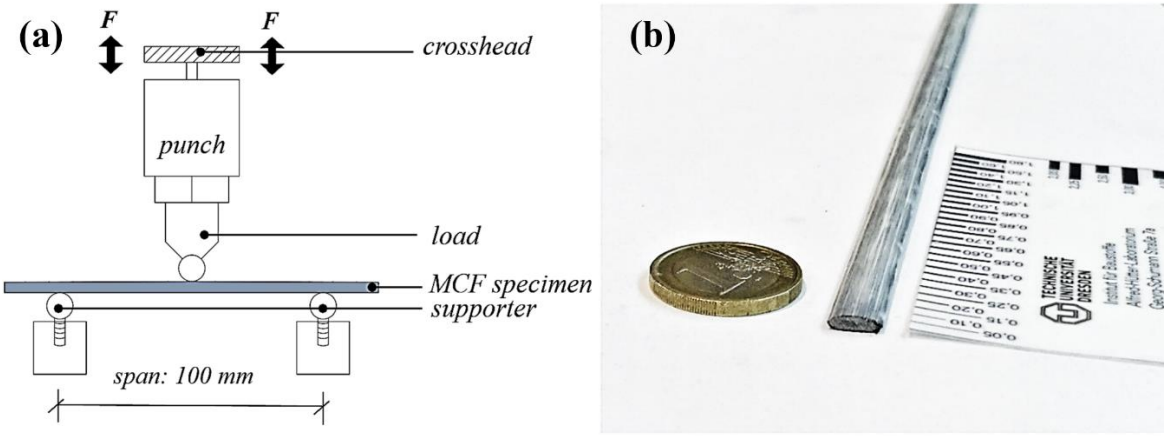

Fig. 3. (a) Scheme of the three-point bending test setup for MCF and (b) ready-made bar of MCF bonded by metakaolin GP.

The tensile strength, Young's modulus, and stress-strain behavior of MCF were assessed by means of uniaxial tension tests at an age of 28 days using the setup sketched in Fig. 4. The tests were performed by means of a servo-hydraulic testing machine EU 20 at ambient temperature. The specimen was loaded by clamping the end anchorages in the grips of the testing machine. The deformations were measured using an electro-optical video extensometer Rudolph XR200 with a precision of ± 0.02 mm and a gauge length of 100 mm positioned in the central area of the samples. Two target marks with black and white stripes were glued onto each sample for this purpose before testing.

Each total specimen length was 600 mm, while the end anchorage length was 100 mm on

each side of the specimen. Thus, the free length of the tested MCF was 400 mm, which meets the requirement of a minimum length of 300 mm and 40 times the bar diameter as specified in ISO 10406-1 [44]. To avoid issues related to local lateral pressure and possible premature failure in the grip regions, the ends of the specimens were strengthened by placing them in aluminum tubes and filling the tubes with epoxy resin. The aluminum tubes had a length of 100 mm, an outer diameter of 12 mm, and an inner diameter of 8.5 mm. The inner parts of the tubes were made with the internal thread to ensure proper bonding with the epoxy resin. The specimen ends were prepared in two steps: (a) Firstly, one end was cast with the epoxy resin in the aluminum tube followed by 24 hours of hardening; (b) subsequently, the specimen was upturned and the second end was strengthened in the same manner.

Uniaxial tension tests of at least ten samples were conducted for each curing duration. Force and deformation were recorded simultaneously in a SIRIUS®HS-STG data acquisition system supplied by DEWEsoft® with a sampling rate of 5000 per second and a filter of 100 HZ.

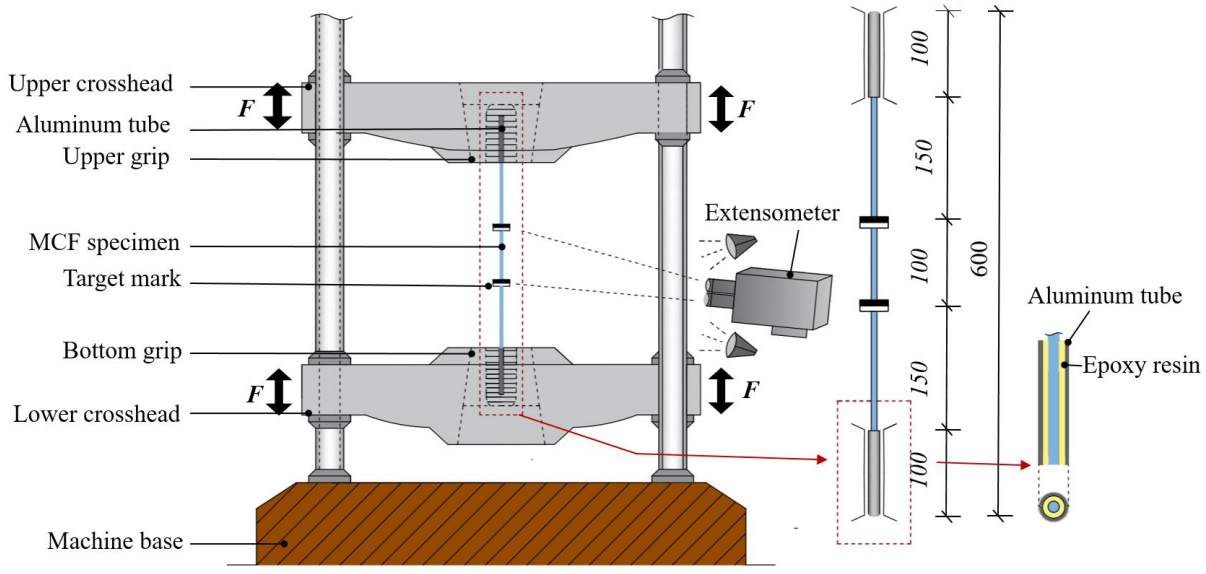

Fig.4. Setup of the uniaxial tension test (dimensions in mm).

2.5 Morphological characterization

The microstructure of MCF was observed using an environmental scanning electron

microscope (ESEM) Quanta 250 FEG from FEI, Eindhoven, the Netherlands, and an optical microscope VHX-6000, Keyence, Neu-Isenburg, Germany, with a high-resolution analysis tool. For porosity evaluations of the MCF and the GP matrices, mercury intrusion porosity (MIP) measurements were conducted on a Porotec Porosimeter PASCAL 140/440 with a mercury surface tension of 0.48 N/m, a contact angle of 140° and testing pressure ranging from 0 to 400.71 MPa. Thermogravimetric analysis (TGA) and differential thermal analysis (DTA) were performed using an STA 409 cell device from Netzsch, Germany, under oxygen atmosphere, operated with a heating rate of 10 K/min from 20 to 1000 °C and 60 ml/min gas flow. Before the analysis, all specimens were exposed to iso-propanol to remove free pore water and were subsequently dried by solvent evaporation.

3. Results and discussion

3.1 Geopolymer matrix characterization

Firstly, properties of the control geopolymer matrix, which was cured at 20 °C, were determined and compared to the specimens exposed to the heat treatment. After 28 days, it exhibits a flexural strength of 7.4 MPa and a compressive strength of 55.2 MPa, displayed as horizontal dashed lines in Fig. 5.

After heat curing, almost all samples were set and hardened, except the samples cured at 50 °C for 2 hours, which did not set sufficiently. Fig. 5 presents the influence of the temperature and duration of curing on the flexural and compressive strength of the geopolymer matrix within the first 8 hours. As expected the elevated temperature accelerates the geopolymerization reaction and thus enables rapid development in strength, especially in the early stage, which is in line with [45–47]. The compressive strengths of the samples cured at 50 °C, and especially at 75 °C, were only slightly lower than the above mentioned 28 d reference value, except for those cured at 50 °C for 2 hours, while the flexural strengths of the thermally treated samples even exceeded that of the references. The early strength increase with rising temperature, here

from 50 to 75 °C, can be traced back to the faster chemical reaction, which is in agreement with the results reported in previous studies [393939,48,49].

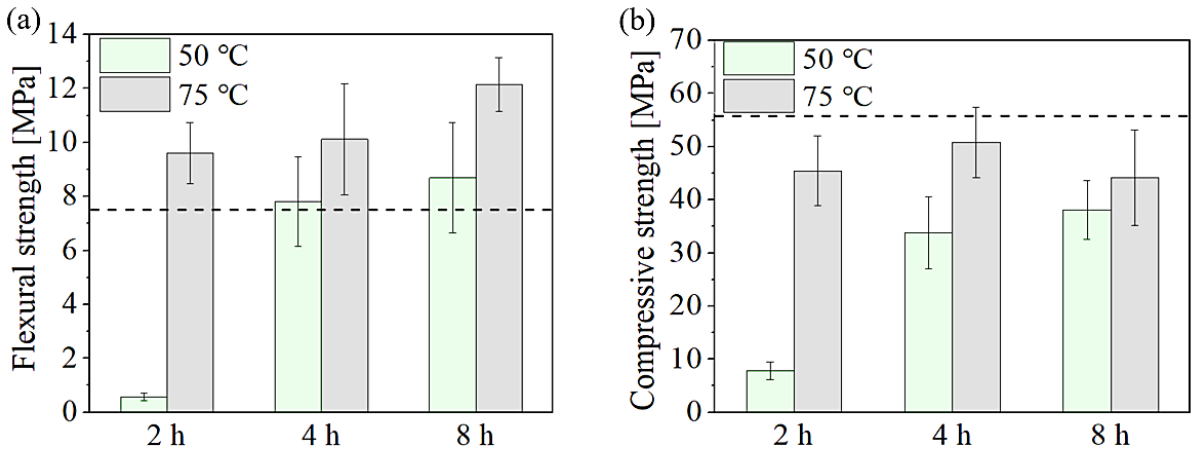

Fig. 5. Influence of thermal treatment on (a) flexural strength and (b) compressive strength of the geopolymer matrix; the horizontal dashed line highlights the reference value obtained for untreated specimens at an age of 28 days.

The longer curing of geopolymer pastes resulted in an increase in flexural strength due to a higher amount of reacted material in the matrix microstructure. This is supported by ESEM observations and is consistent with several previous works as well; cf. Fig. 7 [50–52错误!未定义书签。]. For the lower curing temperature, here 50 °C, the compressive strength development with curing time was found to be similar to that of the flexural strength. At 75 °C, the compressive strength was already significantly high after 2 hours, which further increased slightly for samples cured for 4 hours but then decreased at 8 hours. This decrease in strength might be corroborated by voids formed in the material's microstructure from dissolving MK particles, as identified using ESEM; cf. Fig. 7. Other studies [53–55] reported a similar effect, concluding that the formation of a porous, less compact structure after prolonged curing at elevated temperatures caused the premature failure of the geopolymer under loading. However, it is yet unclear why this change in porosity did not affect the flexural strength in a similar way;

an increase in flexural strength was observed for both temperatures under investigation with increasing duration of curing.

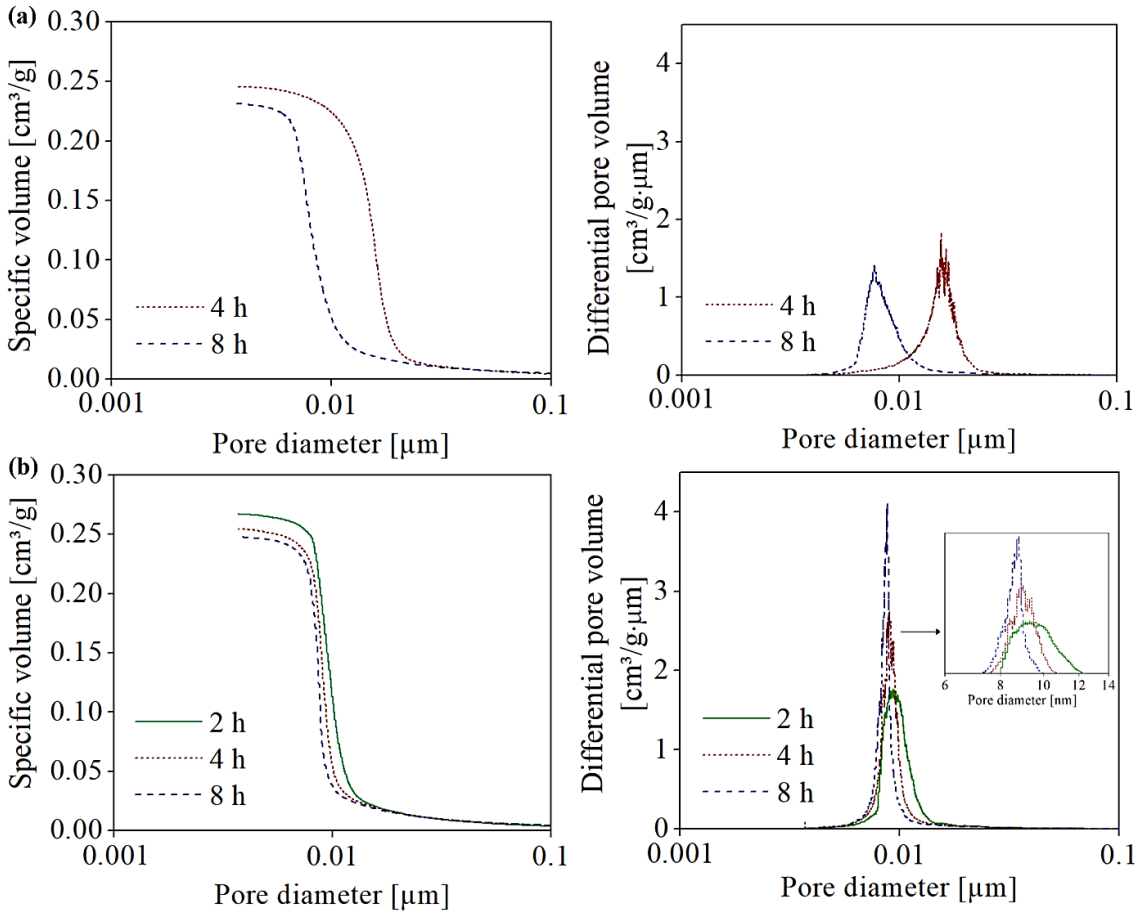

Fig. 6. Cumulative pore volume and pore-size distribution of geopolymer cured (a) at 50 °C and (b) at 75 °C for 2, 4, and 8 hours.

The development of the pore structure in terms of cumulative and differential pore volumes for samples cured at 50 °C and 75 °C at one day is shown in Fig. 6. Note that the lower measurement limit of the pore size in the MIP is 3 nm. Here the principal pore structures are classified into four categories, i.e., nanopores (3 – 10 nm), mesopores (10 – 50 nm), macropores (50 – 200 nm), and pores larger than 200 nm, slightly adjusted from the IUPAC definition [56]. All samples exhibited one prominent peak in pore size distribution, mainly lying between 5 nm and 30 nm in diameter, suggesting regular nano-porosity for GP matrices in general. With longer thermal treatment, the peak at around 0.01 µm in the pore distribution curve becomes

higher and narrower. The samples cured at 50 °C for 2 hours could not be presented in the graphs due to their retarded setting, which hindered accurate measurement.

As shown here in Table 3, the cumulative pore volume of GP matrices yields an increase with rising temperatures from 50 °C to 75 °C, despite the superior mechanical performance of the material treated at 75 °C. This is consistent with the results reported by Rovnaník [4848], who demonstrated that a less ordered structure with poorer quality and more pores are built when the geopolymer mixture is quickly cured at high temperatures.

Table 3. Geopolymer matrix porosities obtained by MIP.

Sample	***Nanopores (3 - 10 nm) [Vol.%]***	***Mesopores (10 - 50 nm) [Vol.%]***	***Macropores (50 - 200 nm) [Vol.%]***	***Larger pores (> 200 nm) [Vol.%]***	***Porosity by Hg-intrusion [Vol.%]***
50 ºC_4 h	3.19	31.54	0.63	0.48	35.84
50 ºC_8 h	26.32	6.29	0.56	0.58	33.71
75 ºC_2 h	21.77	14.32	0.55	0.37	37.01
75 ºC_4 h	29.33	6.61	0.58	0.44	36.98
75 ºC_8 h	30.40	4.35	0.52	0.48	35.75

It is worth noting that both at 50 °C and 75 °C mesopores and macropores in the matrix structure tend gradually to transform themselves into smaller nanopores with rising curing duration (Table 3), suggesting a refinement of the nano-sized pore structure. Prolonged curing promotes the formation of geopolymer gels, which fill the gaps at the nanoscale and thus form a denser and more homogeneous structure [484848]. However, pores can also be generated at elevated temperatures due to excessive water evaporation [53,54535453,57,58]. This process leads after longer curing to a slight increase in the relative number of larger pores, which are more visible in ESEM images; cf. Fig. 7.

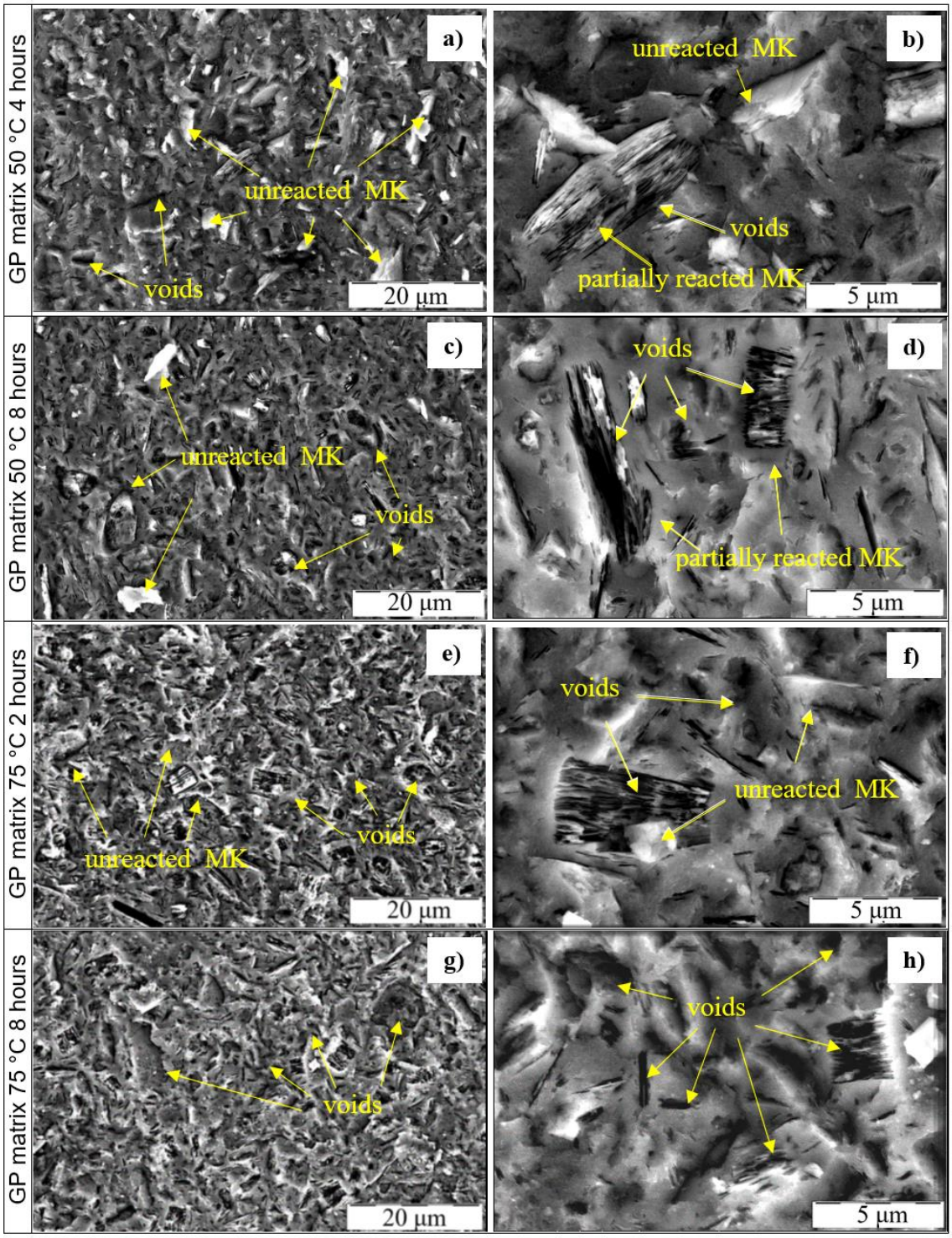

Fig. 7. Microstructure of GP matrices at lower and higher magnification cured at 50 °C (a, b) for 4 hours (c, d), for 8 hours, and cured at 75 °C (e, f) for 2 hours and (g, h) for 8 hours.

The matrices treated at 50 °C show an amorphous binder phase but also unreacted or partially reacted MK particles, as also found in a previous study [40]. When cured for 8 hours,

330 the size and number of unreacted MK particles are clearly reduced, while both the geopolymer
331 gel and void contents slightly increase in the structure; see Fig. 7a-d.
332 At 75 °C after 2 hours of curing, a few unreacted particles could be found, which
333 “disappear” with extended curing; see Fig. 7e-h. However, a more porous microstructure,
334 particularly for samples cured at 75 °C for 8 hours, develops with increasing curing time due to
335 the full dissolution of MK particles as well as subsequent water evaporation. “This increase in
336 porosity could explain the observed slight decrease in compressive strength for this particular
337 parameter combination. Note, the in MIP measured increase in nanopores (3 to 10 nm) cannot
338 be seen and discussed meaningfully at this magnification.”
339 Nevertheless, considering the overall mechanical performance at the early age of the
340 matrices developed, it can be concluded that in the range of parameters investigated the
341 optimum curing temperature for the MCF is 75 °C.
342
343 **3.2 MCF prepared with geopolymer and thermal treatment at 75 °C**
344 Fig. 8 presents the flexural strength obtained from the three-point bending tests on the
345 geopolymer-based MCF immediately after curing at 75 °C as well as after an additional 28 days.
346 Their representative flexural stress-deflection curves are shown in Fig. 9.
347 With increasing duration of curing, a slight increase in flexural strength was found,
348 attributed to the increased degree of geopolymerization. This is in line with the results of the
349 matrices’ mechanical analysis discussed above. In the specimens thermally cured for 8 hours,
350 the early-age flexural strength reached the maximum value of 454 MPa, which is 13% higher
351 than the 28-day flexural strength of the cement-based MCF (402 MPa) developed and tested in
352 prior works at the TU Dresden [14,19], where the same carbon roving was impregnated with a
353 micro-cement-based suspension having a water/binder ratio of 0.8. After storing the specimens
354 for an additional 28 days at standard lab climate (20 °C/55 % RH), the flexural strength among
355 the composites remained still in the same range as the early-age, heat-cured composites and

exhibited a similar increasing trend with extended curing.

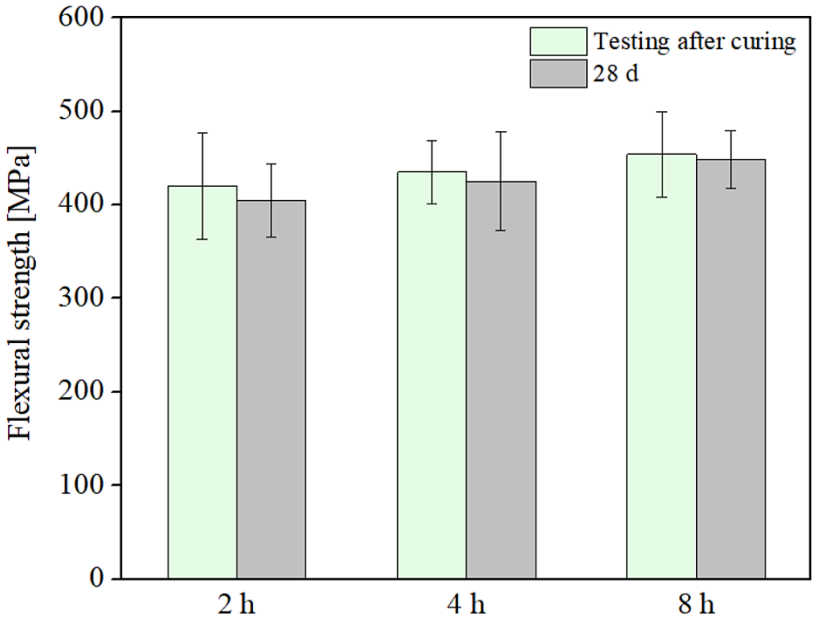

Fig. 8. Flexural strength of MCF tested immediately after curing and at the age of 28 days.

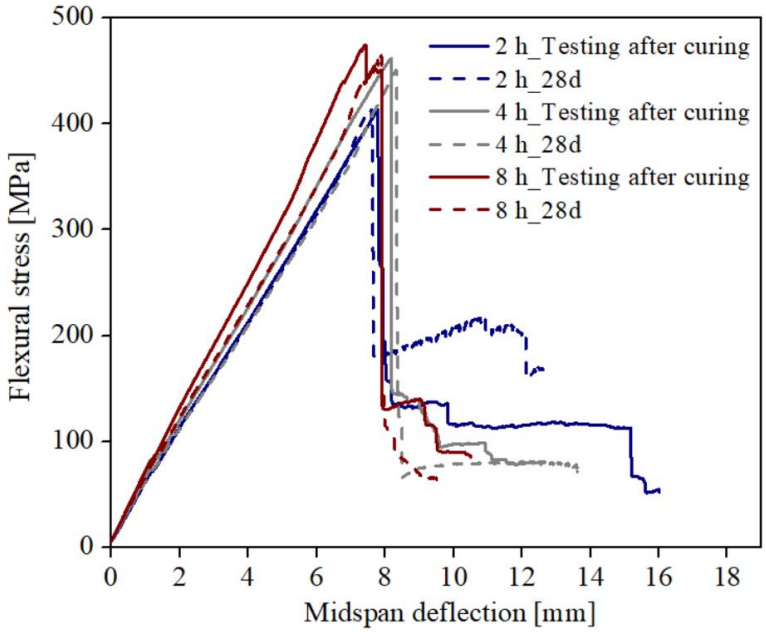

Fig. 9. Representative flexural stress-deflection curves of MCF.

All MCF under investigation yielded an initial, linearly elastic region, followed by a non-linear region; see Fig. 9. After reaching the maximum flexural stress, a sudden drop in stress appears due to the brittle behavior of the geopolymer matrix. In the subsequent non-linear

region, the stress remains stable at lower levels, where crack-bridging and debonding mechanisms play a major role. As shown in Fig. 10, the MCF failure is characterized by the fiber fracture and delamination around broken fibers. For all specimens tested, the main failure process occurred on the compression side, and only a few CFs subjected to tensile stresses were broken on the tension side.

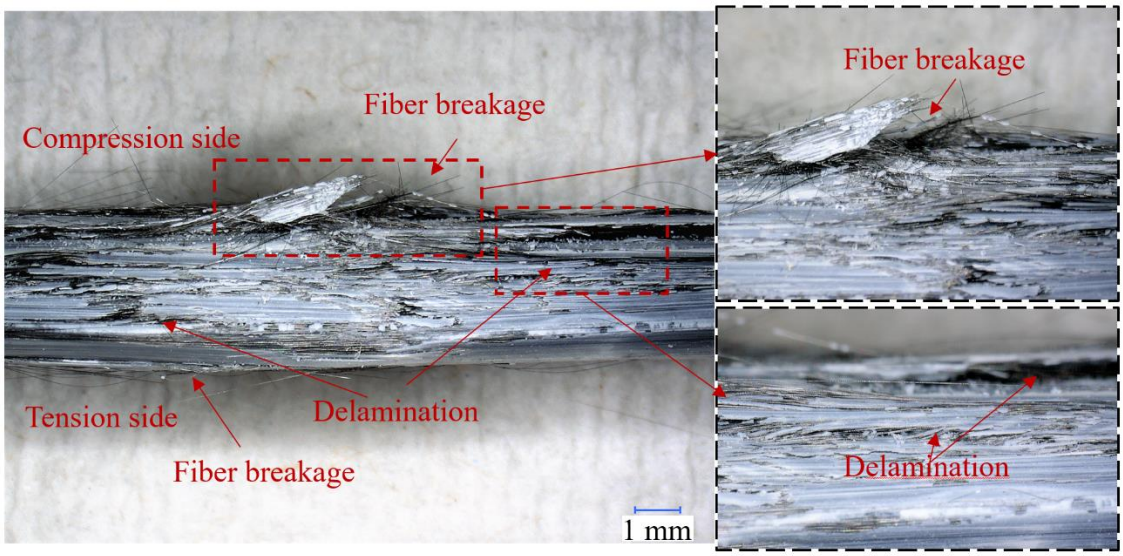

Fig. 10. Typical failure of MCF as observed after a bending test.

Fig. 11 represents the development of the pore structure in terms of cumulative and differential pore volumes for the composites with different curing durations. In general, the porosity of the MCF is significantly influenced not only by the chemical reaction in the matrix, but also by the penetrability of the mineral particles during yarn impregnation [1919,59] and the CF-matrix interaction [60].

Similar to the unreinforced geopolymer samples, the MCF contained a large number of small-sized pores in the range between 4 and 30 nm in their structure; cf. Table 3. Since all MCF were produced with the same device and materials, differences in respect of impregnation quality were deemed negligible.

A comparison from among the porosities of MCF regarding distinct curing regimes appears

challenging since they do not follow a clear tendency, and a number of variables may be influential in this regard. As shown in Table 4, for longer curing, i.e., 4 and 8 hours, the relative number of nanopores seems to increase, seen in the slightly higher peaks at a pore size of approximately 0.01 μm in the pore size distribution. This is in line with other investigations of matrices and can be traced back to a higher degree of geopolymerization and densification at the nanoscale; cf. Fig. 6. However, in general the differences are very small, seen also in the cumulative porosity. Hence, the significance of pore size distribution analysis is limited in this regard.

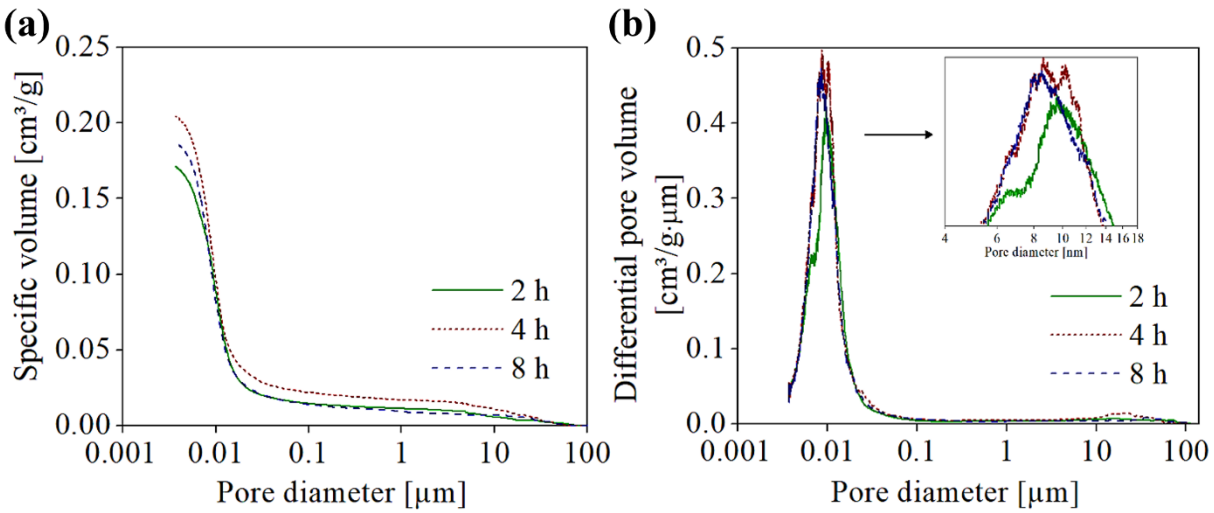

Fig. 11. (a) Cumulative pore volume and (b) pore-size distribution in the geopolymer-based MCFs after thermal curing at 75 ºC.

Table 4. MCF porosities obtained by MIP.

Sample	***Nanopores (3 - 10 nm) [Vol.%]***	***Mesopores (10 - 50 nm) [Vol.%]***	***Macropores (50 - 200 nm) [Vol.%]***	***Larger pores (> 200 nm) [Vol.%]***	***Porosity by Hg-intrusion [Vol.%]***
75 ºC_2 h	14.14	11.98	0.70	2.29	29.10
75 ºC_4 h	15.97	10.45	0.79	2.98	30.19
75 ºC_8 h	15.82	9.68	0.74	1.85	28.09

For investigating the ability of this new reinforcement material to withstand tension, the

ultimate tensile stress σ_{max} and Young's modulus E of the MCF were examined. Since all MCF were manufactured with the same device and material composition, the fiber volume fraction for each curing duration is identical in each sample, approximately 13% (cf. TGA analysis). The tensile strength was calculated by dividing the maximum tensile force by the sum of all carbon filament cross-section areas of the impregnated yarn, which is a common procedure to characterize the yarn strand and textile reinforcement under uniaxial tensile loading for carbon textile-reinforced concrete [61–63]. The Young's modulus was calculated from the stress-strain diagram as the secant modulus between the load levels at 20% and 70% of the tensile capacity in the elastic phase and obtained using Eq. (2):

$$E = \frac{0.7\ \sigma_{max} - 0.2\ \sigma_{max}}{\varepsilon_{0.7\ \sigma_{max}} - \varepsilon_{0.2\ \sigma_{max}}} \quad (2)$$

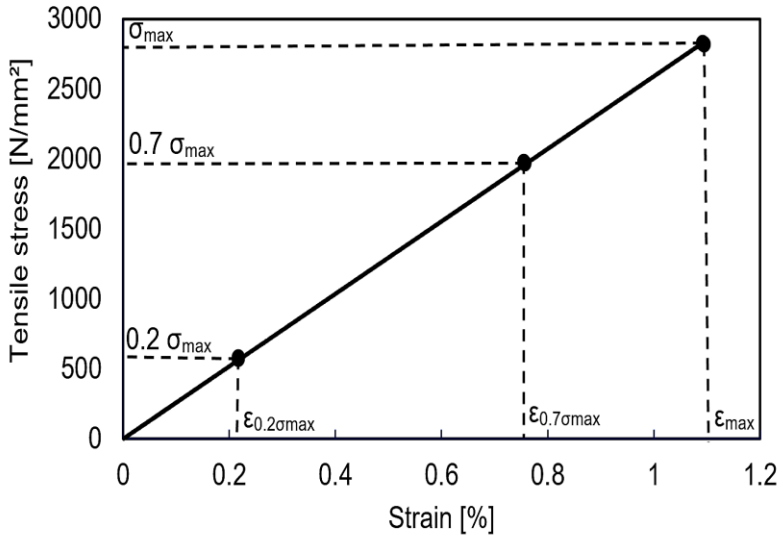

Fig. 12. Graphic representation of a typical tensile stress-strain curve for MCF.

The schematic representation of the typical tensile stress-strain curve depicted in Fig. 12 shows a linearly increasing trend and failure upon reaching the ultimate stress, without an intermediate yielding point, signifying a brittle material behaviour. As observed by ESEM, cf. Fig. 16, the carbon filaments were well embedded into the geopolymer matrix, which ensures sufficient shear force transfer capacity from the outer to the inner filaments under tensile loading. Thus,

the failure of the impregnated yarn is, rather than by slippage, mainly dominated by the breakage of the filaments within the gauge length of the specimen; see Fig. 13.

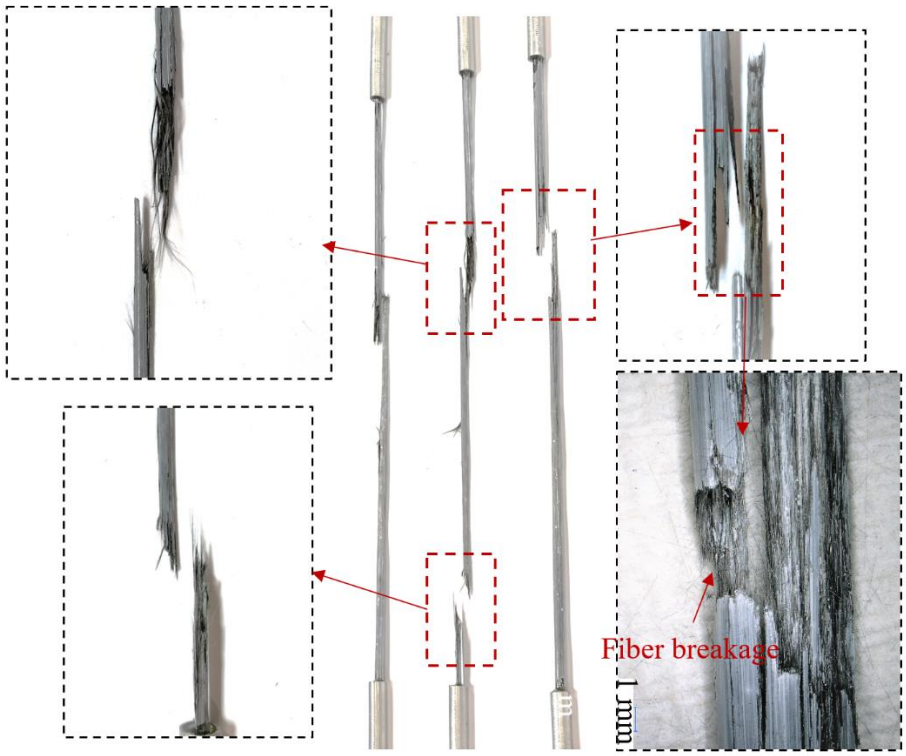

Fig. 13. Failed MCF specimens after the tensile test.

Table 5 exhibits the results of the uniaxial tension tests of the geopolymer-based MCFs. With an increase in the duration of curing, the tensile strength and Young's modulus of the specimens tend to increase steadily, reaching maximum values of 2960 MPa and 259 GPa, respectively, at a curing duration of 8 hours. These are also higher than the 28-day tensile strength and elastic modulus of the cement-based MCF, i.e., 2250 MPa and 225 GPa, respectively [14]. Longer thermal curing of the composite supported the reactivity of the matrix and so contributed to the increase in the matrix strength, as already discussed above, which results in increases in tensile strength, Young's Modulus, and strain to rupture for the MCF.

Table 5. Average tensile properties of geopolymer-based MCF thermally treated at 75 °C; standard deviations are given in parentheses.

Curing time	*Tensile strength [MPa]*	*Failure strain [%]*	*Young's modulus [GPa]*
2 h	2607 (179)	0.97 (0.07)	243 (12)
4 h	2736 (153)	1.04 (0.08)	252 (19)
8 h	2960 (55)	1.05 (0.09)	259 (3)

3.3 Chemical and morphological analysis

From the results of the mechanical tests, it can be concluded that the elevated temperature accelerated the geopolymerization, which enhanced the load-bearing capacity from the matrix to the CF yarn. To support these macro-mechanical findings, the composites were thermally and morphologically characterized.

The results of thermogravimetric analysis (TGA) for MCF treated at 75 °C for 2 and 8 hours are shown in Fig. 14. They indicate similar behavior for both specimens with respect to loss of mass, with small differences only. Independent of the curing duration of MCF, an initial significant weight loss in the range of 60 ºC to 250 ºC can be seen, which is in line with the results reported in the literature [64,65]. The mass loss at these temperatures is attributed to both freely evaporable and chemically bonded water; the latter can be easily removed from the potassium silicate gel structure [66–68], pointing to endothermal reactions; see Fig. 15. Considering the DTG curves in this specific temperature range, the composites with a shorter curing time of 2 hours yield a higher rate of dehydration below 100 ºC, a consequence of their higher amount of evaporable water. Extended durations of curing, i.e., 2 to 8 hours, caused a shift of the first weight loss peak to higher temperatures from 135 °C to 147 °C, indicating again a higher degree of geopolymerization and a denser and stabler microstructure. The dehydration of this specific aluminum-silicate gel required more energy, as also reflected in DTA curves. For the 8 h-treated sample, a wider endothermic peak was observed, which is additionally

shifted to a higher temperature, namely 147 ºC.

The second significant loss of mass in the TG curve is found in the range from 450 °C to 650 ºC, mainly attributed to the oxidation of the CFs. This particular mass loss indicates carbon fiber mass and volume contents of approximately 15.4 % and 13 %, respectively. Moreover, also dehydroxylation of hydroxyl groups of the matrix occurred in this temperature region. Above 300 ºC, the weight loss of the matrix is associated with dehydroxylation through the silanol and aluminol groups' condensation, which is completed before the temperature reaches 850 ºC [40 **错误!未定义书签。**].

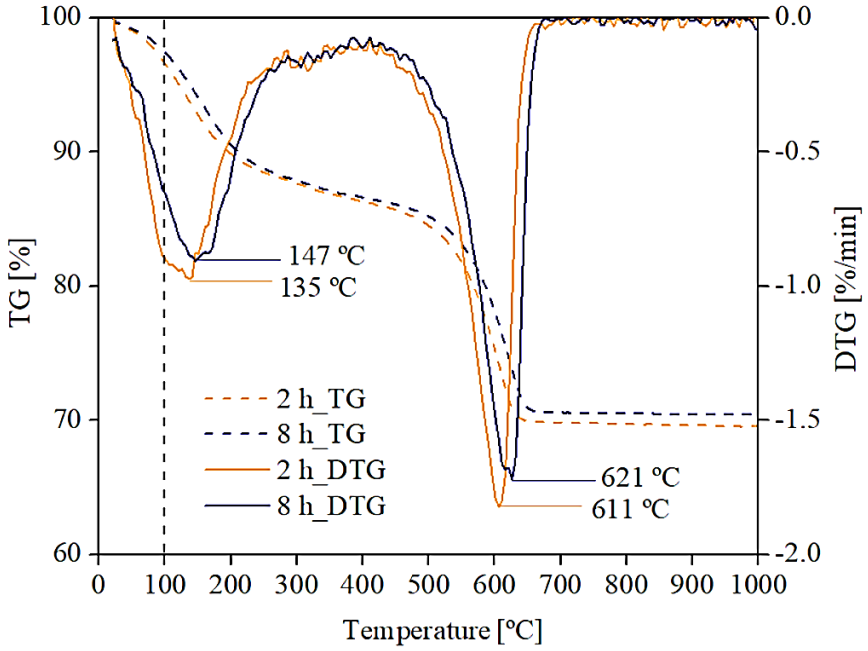

Fig. 14. TG/DTG curves for the geopolymer-based MCF cured at 75 ºC for 2 hours and 8 hours.

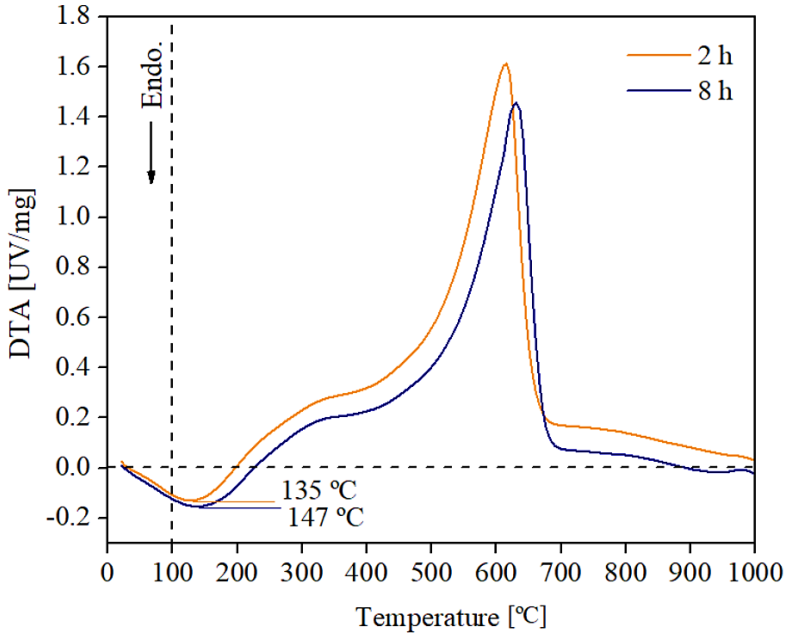

Fig. 15. DTA curves for the geopolymer based MCF cured at 75 °C for 2 and 8 hours.

The morphological features of MCF confirm the aspects discussed above. Fig. 16a and Fig. 16b show an optical microscopic image and an ESEM image, respectively, of the cross-section of the embedded yarn. The cross-section was prepared by perpendicularly cutting a composite specimen cured over 8 hours. Since all specimens were produced with the same material composition and device, they possess the same impregnation quality and the fiber-matrix distribution over the composite cross-section. Hence, the images are representative as well for specimens produced with the other two curing durations. The black circles in Fig. 16b indicate the positioning of single carbon filaments. Obviously, the filaments were uniformly distributed in the impregnating geopolymer matrix, indicating the high degree of the suspension's penetration into the entire yarn. Only a few accumulations of the impregnation matrix without embedded filaments could be found. The good embedment of the carbon filaments within the matrix enables efficient shear-stress transfer between them, thus resulting in the high mechanical performance of the composite.

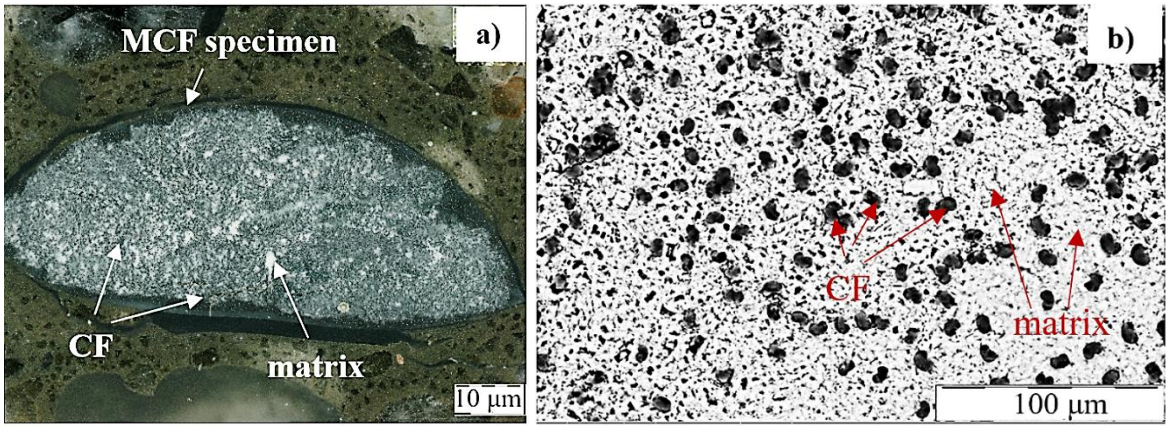

Fig. 16. Microscopic images showing the cross-section of MCF cured at 75 °C for 8 hours at (a) lower magnification (optical microscope image) and (b) higher magnification (ESEM image).

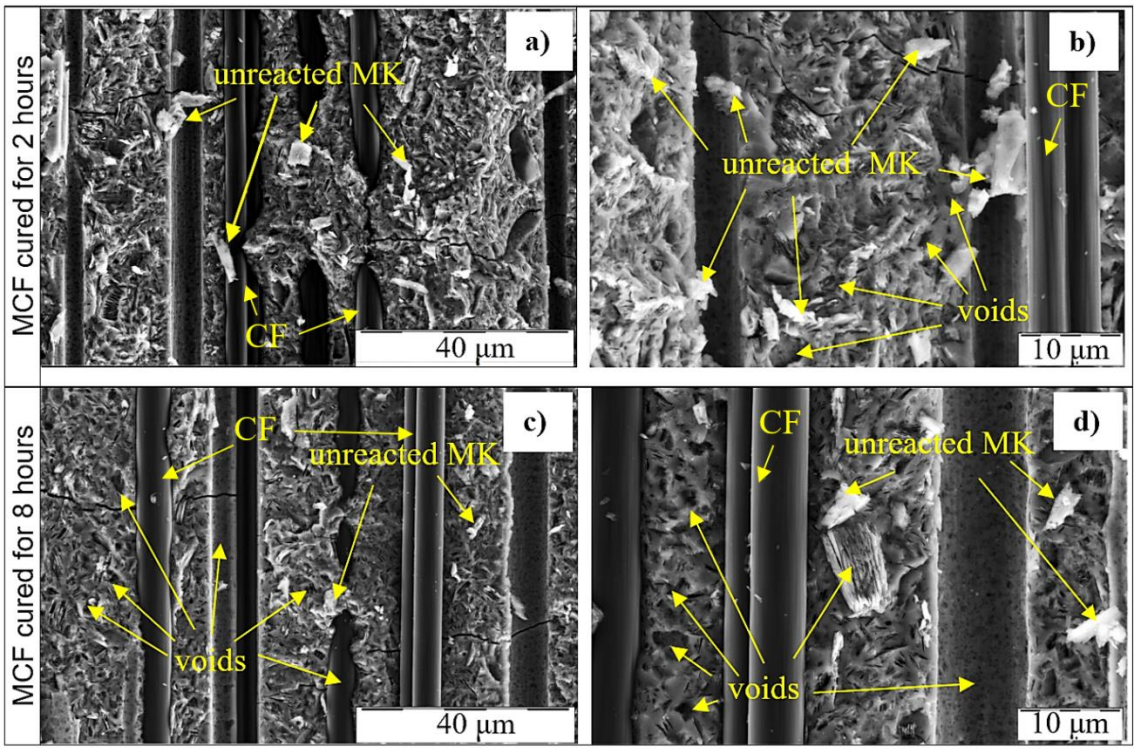

Fig. 17. ESEM images of split MCF cured at 75 °C (a, b) for 2 hours and (c, d) for 8 hours, each pairwise with lower and higher magnification, respectively.

Fig. 17 provides an insight into the interfaces' morphology by exhibiting MCF specimens split in the direction of the fibers. Continuous fiber embedment without any distinct gaps can

be observed, indicating good physical interaction among the components. Similar to unreinforced geopolymer samples, the composites yielded a high proportion of relatively large, non-reacted or partially reacted MK after the short curing duration of 2 hours, suggesting a lower extent of geopolymerization. Contrarily, with curing extended to 8 hours, fewer unreacted particles and more aluminosilicate gel are visible. This is likely to contribute to more uniform network formation, subsequently to higher strength of the matrix, and hence to improve filament embedment. However, more cavities were formed on the surface of partially reacted particles and in the gel area after longer curing, resulting in a more porous microstructure.

Conclusions

The production of mineral-impregnated, carbon fiber composites (MCF) using a metakaolin-made geopolymer suspension is a new approach conceived to enable a continuous, automated manufacturing process subject to controlled thermal curing. At ambient temperature, the setting of the geopolymer impregnation matrix is slowed down to ensure a sufficient processing window of several hours for a continuous production with such matrices.

To determine optimal post-treatment conditions for composite production, the investigation focused firstly on the development of compressive and flexural strength of the geopolymer matrix. The samples were subjected to curing under elevated temperatures of 50 °C and 75 ºC over short periods of 2 to 8 hours. Higher curing temperature of 75 ºC and a longer curing duration of 8 hours were found to yield the highest geopolymer matrix strength in the early stage, whilst causing a slightly more porous matrix microstructure.

Subsequently, the MCF were reproducibly manufactured with oven curing at 75 ºC, and their mechanical and morphological properties were assessed. The thermal activation contributed to very fast setting and rapid early strength development of the MCF within mere hours. Prolonged curing considerably promoted the geopolymerization and thus gradually increased both the early-age strength and the 28-day strength of MCF, as observed in the

bending and uniaxial tension tests. After thermal curing of 8 hours, the composites achieved a high flexural strength of 454 MPa, a tensile strength of 2960 MPa, and an elastic modulus of 259 GPa, pointing to superior mechanical properties in comparison with the 28 day-strength of cement-based MCF previously developed by the authors. The morphological investigation validated the high quality of impregnation, i.e., the good embedment of the filaments and the resulting efficient stress-transfer within the bundle under loading.

In summary, the excellent properties of this newly developed reinforcement material at early ages deliver very great flexibility with regard to automated production, and after thermal curing high mechanical performance for various structural applications.

Acknowledgment

This research is funded by the European Social Fund and co-financed by tax funds based on the budget approved by the members of the Saxon State Parliament under project LIP/KAKO 2019_TUD (No. 100380876). Moreover, the authors acknowledge the financial support of the Brazilian organizations CNPq and CAPES and by the German Academic Exchange Service (DAAD) as well for funding the project, numbered 8887.144079/2017-00.

References

[1] A. Scholzen, R. Chudoba, J. Hegger, Dünnwandiges Schalentragwerk aus textilbewehrtem Beton: Entwurf, Bemessung und baupraktische Umsetzung, Beton- Und Stahlbetonbau. 107 (2012) 767–776.
[2] S. Scheerer, Was ist Textilbeton?: Eine kurze Einführung in das Thema, Beton- Und Stahlbetonbau. 110 (2015) 4–7.
[3] R. Böhm, M. Thieme, D. Wohlfahrt, D.S. Wolz, B. Richter, H. Jäger, Reinforcement systems for carbon concrete composites based on low-cost carbon fibers, Fibers. 6(3) (2018) 56.
[4] C.E. Bakis, L.C. Bank, V.L. Brown, E. Cosenza, J.F. Davalos, J.J. Lesko, A. Machida, S.H. Rizkalla, T.C. Triantafillou, Fiber-reinforced polymer composites for construction - State-of-the-art review, J. Compos. Constr. 6 (2002) 73–87.
[5] L.C. Hollaway, A review of the present and future utilisation of FRP composites in the civil infrastructure with reference to their important in-service properties, Constr. Build. Mater. 24 (2010) 2419–2445.
[6] U. Köckritz, P. Offermann, F. Jesse, M. Curbach, Influence of textile manufacturing technology on load bearing behavior of textile reinforced concrete, in: Proc. 13th Int. Techtextile-Symp., 2005.
[7] F. Jesse, M. Curbach, Verstärken mit Textilbeton, Wiley Online Library, 2010.
[8] K. Schneider, A. Michel, M. Liebscher, V. Mechtcherine, Bond behavior of mineral-impregnated and polymer-impregnated reinforcement structures made of carbon fibres at temperatures up to 500 °C. Beton- und Stahlbetonbau. 113 (2018) 886-894.
[9] F. de Andrade Silva, M. Butler, S. Hempel, R.D. Toledo Filho, V. Mechtcherine, Effects of elevated temperatures on the interface properties of carbon textile-reinforced concrete, Cem. Concr. Compos. 48 (2014) 26–34.
[10] A. Katz, N. Berman, Modeling the effect of high temperature on the bond of FRP reinforcing bars to concrete, Cem. Concr. Compos. 22 (2000) 433–443.
[11] R.J. Hamad, M.M. Johari, R.H. Haddad, Mechanical properties and bond characteristics of different fiber reinforced polymer rebars at elevated temperatures, Constr. Build. Mater. 142 (2017) 521–535.
[12] A. Katz, N. Berman, L.C. Bank, Effect of high temperature on bond strength of FRP rebars, J. Compos. Constr. 3 (1999) 73–81.
[13] A. Younes, A. Seidel, T. Engler, C. Cherif, D. Ehlig, Mechanical behaviour of carbon and glass filament yarns under high temperatures for composite applications, J. Text. Inst. 104 (2013) 251–259.
[14] V. Mechtcherine, A. Michel, M. Liebscher, K. Schneider, C. Großmann, Mineral-impregnated carbon fiber composites as novel reinforcement for concrete construction: Material and automation perspectives, Autom. Constr. 110 (2020) 103002.
[15] V. Mechtcherine, A. Michel, M. Liebscher, T. Schmeier, Extrusion-Based Additive Manufacturing with Carbon Reinforced Concrete: Concept and Feasibility Study, Materials (Basel). 13 (2020) 2568.
[16] J. Zhao, M. Liebscher, A. Michel, K. Schneider, R. Foest, M. Fröhlich, A. Quade, V. Mechtcherine, Plasma-generated silicon oxide coatings of carbon fibres for improved bonding to mineral-based impregnation materials and concrete matrices, Cem. Concr. Compos. (2020) 103667.
[17] R. Nadiv, A. Peled, V. Mechtcherine, S. Hempel, C. Schroefl, Micro- and nanoparticle mineral coating for enhanced properties of carbon multifilament yarn cement-based composites, Compos. Part B Eng. 111 (2017) 179–189.
[18] A. Badanoiu, J. Holmgren, Cementitious composites reinforced with continuous carbon fibres for strengthening of concrete structures, Cem. Concr. Compos. 25 (2003) 387–394.

[19] K. Schneider, A. Michel, M. Liebscher, L. Terreri, S. Hempel, V. Mechtcherine, Mineral-impregnated carbon fibre reinforcement for higsh temperature resistance of thin-walled concrete structures, Cem. Concr. Compos. 97 (2019) 68–77.
[20] A. Zhang, X. Gao, The Feasibility of Modified Magnesia-Phosphate Cement as a Heat Resistant Adhesive for Strengthening Concrete with Carbon Sheets, Appl. Sci. 6 (2016) 178.
[21] P. Duxson, S.W. Mallicoat, G.C. Lukey, W.M. Kriven, J.S.J. van Deventer, The effect of alkali and Si/Al ratio on the development of mechanical properties of metakaolin-based geopolymers, Colloids Surfaces A Physicochem. Eng. Asp. 292 (2007) 8–20.
[22] P. Duxson, J.L. Provis, G.C. Lukey, S.W. Mallicoat, W.M. Kriven, J.S.J. Van Deventer, Understanding the relationship between geopolymer composition, microstructure and mechanical properties, Colloids Surfaces A Physicochem. Eng. Asp. 269 (2005) 47–58.
[23] V.F.F. Barbosa, K.J.D. MacKenzie, Thermal behaviour of inorganic geopolymers and composites derived from sodium polysialate, Mater. Res. Bull. 38 (2003) 319–331.
[24] R.A. Sá Ribeiro, M.G. Sá Ribeiro, W.M. Kriven, Review of particle- and fiber-reinforced metakaolin-based geopolymer composites, J. Ceram. Sci. Technol. 8 (2017) 307–321.
[25] F.U.A. Shaikh, Review of mechanical properties of short fibre reinforced geopolymer composites, Constr. Build. Mater. 43 (2013) 37–49.
[26] T. Lin, D. Jia, P. He, M. Wang, D. Liang, Effects of fiber length on mechanical properties and fracture behavior of short carbon fiber reinforced geopolymer matrix composites, Mater. Sci. Eng. A. 497 (2008) 181–185.
[27] N. Ranjbar, M. Zhang, Fiber-reinforced geopolymer composites: A review, Cem. Concr. Compos. 107 (2020) 103498.
[28] M. Welter, M. Schmücker, K.J.D. MacKenzie, Evolution of the fibre-matrix interactions in basalt-fibre-reinforced geopolymer-matrix composites after heating, J. Ceram. Sci. Technol. 6 (2015) 17–24.
[29] D.H. Tran, P. Louda, O. Bortnovsky, P. Bezucha, Effect of Curing Temperature on Flexural Properties of Silica-Based Geopolymer-Carbon Reinforced Composite, Manuf. Eng. 37 (2009) 492–497.
[30] P. He, D. Jia, T. Lin, M. Wang, Y. Zhou, Effects of high-temperature heat treatment on the mechanical properties of unidirectional carbon fiber reinforced geopolymer composites, Ceram. Int. 36 (2010) 1447–1453.
[31] T. Doan, P. Louda, D. Kroisova, O. Bortnovsky, N. Thang, New Generation of Geopolymer Composite for Fire-Resistance, Adv. Compos. Mater. - Anal. Nat. Man-Made Mater. (2011).
[32] C. Menna, D. Asprone, C. Ferone, F. Colangelo, A. Balsamo, A. Prota, R. Cioffi, G. Manfredi, Use of geopolymers for composite external reinforcement of RC members, Compos. Part B Eng. 45 (2013) 1667–1676.
[33] C. Ferone, F. Colangelo, G. Roviello, D. Asprone, C. Menna, A. Balsamo, A. Prota, R. Cioffi, G. Manfredi, Application-oriented chemical optimization of a metakaolin based geopolymer, Materials (Basel). 6 (2013) 1920–1939.
[34] J. Davidovits, Geopolymers and geopolymeric materials, J. Therm. Anal. 35 (1989) 429–441.
[35] R.B. Holland, K.E. Kurtis, L.F. Kahn, Effect of different concrete materials on the corrosion of the embedded reinforcing steel, Elsevier Ltd, 2016.
[36] B. Nematollahi, J. Sanjayan, Effect of different superplasticizers and activator combinations on workability and strength of fly ash based geopolymer, Mater. Des. 57 (2014) 667–672.
[37] SIGRAFIL® Continuous Carbon Fiber Tows, SIGRAFIL®. https://www.sglcarbon.com/en/markets-solutions/material/sigrafil-continuous-carbon-fiber-tows/, accessed April 2020.

[38] A.C. Constâncio Trindade, I. Curosu, M. Liebscher, V. Mechtcherine, F. de Andrade Silva, On the mechanical performance of K- and Na-based strain-hardening geopolymer composites (SHGC) reinforced with PVA fibers, Constr. Build. Mater. 248 (2020) 118558.
[39] Muhd Fadhil Nurruddin, I.G.S. Sani Haruna, Bashar S. Mohammed, Methods of curing geopolymer concrete: A review, Int. J. Adv. Appl. Sci. 5 (2018) 31–36.
[40] J.L. Bell, P.E. Driemeyer, W.M. Kriven, Formation of ceramics from metakaolin-based geopolymers. Part II: K-based geopolymer, J. Am. Ceram. Soc. 92 (2009) 607–615.
[41] A.C.C. Trindade, F.A. Silva, H.A. Alcamand, P.H.R. Borges, On the durability behavior of natural fiber reinforced geopolymers, in: Ceram. Eng. Sci. Proc., 2018: pp. 215–228.
[42] DIN EN 12390-5, Testing hardened concrete - Part 5: Flexural strength of test specimens, German Institute for Standardisation, 2009.
[43] DIN EN 12390-3, Testing hardened concrete – Part 3: Compressive strength of test specimens, German Institute for Standardisation, 2009.
[44] ISO 10406-1, Fibre-reinforced polymer (FRP) reinforcement of concrete – Test Methods, Part 1: FRP bars and grids, International Organization for Standardization, Switzerland, 2008.
[45] L. Chen, Z. Wang, Y. Wang, J. Feng, Preparation and properties of alkali activated metakaolin-based geopolymer, Materials (Basel). 9 (2016) 767.
[46] M.S. Muñiz-Villarreal, A. Manzano-Ramírez, S. Sampieri-Bulbarela, J.R. Gasca-Tirado, J.L. Reyes-Araiza, J.C. Rubio-Ávalos, J.J. Pérez-Bueno, L.M. Apatiga, A. Zaldivar-Cadena, V. Amigó-Borrás, The effect of temperature on the geopolymerization process of a metakaolin-based geopolymer, Mater. Lett. 65 (2011) 995–998.
[47] T.A. García-Mejía, M. de Lourdes Chávez-García, Compressive Strength of Metakaolin-Based Geopolymers: Influence of KOH Concentration, Temperature, Time and Relative Humidity, Mater. Sci. Appl. 07 (2016) 772–791.
[48] P. Rovnaník, Effect of curing temperature on the development of hard structure of metakaolin-based geopolymer, Constr. Build. Mater. 24 (2010) 1176–1183.
[49] Y.M. Liew, H. Kamarudin, A.M.M. Al Bakri, M. Bnhussain, M. Luqman, I.K. Nizar, C.M. Ruzaidi, C.Y. Heah, Effect of curing regimes on metakaolin geopolymer pastes produced from geopolymer powder, in: Adv. Mater. Res., 2013: pp. 931–936.
[50] B.S. Manesh, S.M. B, W.M. R, P.S. V, Effect of Duration and Temperature of Curing on Compressive Strength of Geopolymer Concrete, Int. J. Eng. Innov. Technol. 1 (2012) 152–155.
[51] P. Sturm, G.J.G. Gluth, S. Simon, H.J.H. Brouwers, H.C. Kühne, The effect of heat treatment on the mechanical and structural properties of one-part geopolymer-zeolite composites, Thermochim. Acta. 635 (2016) 41–58.
[52] R. Dirgantara, Development of Brown Coal Fly Ash Geopolymer Concrete. Doctoral dissertation, RMIT University, (2016).
[53] F.G.M. Aredes, T.M.B. Campos, J.P.B. MacHado, K.K. Sakane, G.P. Thim, D.D. Brunelli, Effect of cure temperature on the formation of metakaolinite-based geopolymer, Ceram. Int. 41 (2015) 7302–7311.
[54] Y. Luna-Galiano, C. Fernández-Pereira, M. Izquierdo, Contributions to the study of porosity in fly ash-based geopolymers. Relationship between degree of reaction, porosity and compressive strength, Mater. Constr. 66 (324) (2016) e098.
[55] J.G.S. Van Jaarsveld, J.S.J. Van Deventer, G.C. Lukey, The effect of composition and temperature on the properties of fly ash- and kaolinite-based geopolymers, Chem. Eng. J. 89 (2002) 63–73.
[56] J. Rouquerol, G. Baron, R. Denoyel, H. Giesche, J. Groen, P. Klobes, P. Levitz, A. V. Neimark, S. Rigby, R. Skudas, K. Sing, M. Thommes, K. Unger, Liquid intrusion and

alternative methods for the characterization of macroporous materials (IUPAC technical report), Pure Appl. Chem. 84 (2012) 107–136.
[57] P. Chindaprasirt, T. Chareerat, V. Sirivivatnanon, Workability and strength of coarse high calcium fly ash geopolymer, Cem. Concr. Compos. 29 (2007) 224–229.
[58] K. Zulkifly, H.C. Yong, M.M.A.B. Abdullah, L.Y. Ming, D. Panias, K. Sakkas, Review of Geopolymer Behaviour in Thermal Environment, in: IOP Conf. Ser. Mater. Sci. Eng. 209(1) (2017) 012085.
[59] R. Nadiv, A. Peled, V. Mechtcherine, S. Hempel, C. Schroefl, Micro- and nanoparticle mineral coating for enhanced properties of carbon multifilament yarn cement-based composites, Compos. Part B Eng. 111 (2017) 179–189.
[60] K. Schneider, M. Lieboldt, M. Liebscher, M. Fröhlich, S. Hempel, M. Butler, C. Schröfl, V. Mechtcherine, Mineral-based coating of plasma-treated carbon fibre rovings for carbon concrete composites with enhanced mechanical performance, Materials. 10 (2017) 360.
[61] E. Schütze, J. Bielak, S. Scheerer, J. Hegger, M. Curbach, Einaxialer Zugversuch für Carbonbeton mit textiler Bewehrung, Beton- Und Stahlbetonbau. 113 (2018) 33–47.
[62] T. Gong, A.A. Heravi, G. Alsous, I. Curosu, V. Mechtcherine, The impact-tensile behavior of cementitious composites reinforced with carbon textile and short polymer fibers, Appl. Sci. 9 (19) (2019) 4048.
[63] S. Rempel, M. Ricker, Ermittlung der Material kenn werte der Bewehrung für die Bemessung von textilbewehrten Bauteilen, Bauingenieur. 92 (2017) 280–288.
[64] H.Y. Zhang, V. Kodur, B. Wu, L. Cao, S.L. Qi, Comparative thermal and mechanical performance of geopolymers derived from metakaolin and fly ash, J. Mater. Civ. Eng. 28 (2) (2016) 04015092.
[65] C.A. Rosas-Casarez, S.P. Arredondo-Rea, J.M. Gómez-Soberón, J.L. Alamaral-Sánchez, R. CorralHiguera, M.J. Chinchillas-Chinchillas, O.H. Acuña-Agüero, Experimental study of XRD, FTIR and TGA techniques in geopolymeric materials, Int. J. Adv. Comput. Sci. Its Appl. 4 (2014) 25-30.
[66] P. Duxson, G.C. Lukey, J.S.J. van Deventer, Thermal evolution of metakaolin geopolymers: Part 1 - Physical evolution, J. Non. Cryst. Solids. 352 (2006) 5541–5555.
[67] P. Duxson, G.C. Lukey, J.S.J. Van Deventer, Physical evolution of Na-geopolymer derived from metakaolin up to 1000 °c, J. Mater. Sci. 42 (2007) 3044–3054.
[68] S.A. Bernal, E.D. Rodríguez, R. Mejía De Gutiérrez, M. Gordillo, J.L. Provis, Mechanical and thermal characterisation of geopolymers based on silicate-activated metakaolin/slag blends, J. Mater. Sci. 46 (2011) 5477–5486.